

# Effects of volume on travel distance of mass movements triggered by the 2005 Kashmir earthquake, in the Northeast Himalayas of Pakistan

Muhammad Basharat · Joachim Rohn

Received: 31 August 2013 / Accepted: 3 January 2015 / Published online: 15 January 2015  
© Springer Science+Business Media Dordrecht 2015

**Abstract** The 2005 Kashmir earthquake ( $M_w$  7.6) generated widespread mass movements in the Northeast Himalayas of Pakistan. The mass movements were mainly catastrophic rock avalanches, rockslides, rockfalls and debris falls, ranging in volume from a few hundred cubic meters to hundreds of million cubic meters. Data of 103 mass movement events were collected during field surveys to characterize each event. The mass movements and their travel distances were analyzed, using empirical models, widely adopted in the literature. The empirical approaches were used to analyze the relationships between geometrical parameters like volume, Fahrböschung angle, fall height, surface area, travel path and travel distance. The mobility of mass movements was expressed as the ratio between the height of fall and travel distance as function of volume. The volume was estimated by multiplying the deposit area by average thickness. The Fahrböschung angle showed a decreasing tendency with increasing mass movement volume. In addition, the Fahrböschung angle of mass movements with small volumes was more variable. A strongly correlated linear trend exists between the height of fall and travel distance for all types of the mass movement. Moreover, a weak correlation was found between unconfined and partly confined travel path. The empirical results of the 2005 Kashmir earthquake data are consistent with the previously published data from other parts of the world.

**Keywords** Mass movement · Kashmir earthquake · Volume · Travel distance · Fahrböschung angle

---

M. Basharat (✉)  
Institute of Geology, University of Azad Jammu and Kashmir, Muzaffarabad 13100, Pakistan  
e-mail: basharatgeo@yahoo.com

M. Basharat · J. Rohn  
GeoZentrum Nordbayern, Friedrich-Alexander-University Erlangen-Nuremberg, 91054 Erlangen,  
Germany

## 1 Introduction

The mass movement is a significant phenomenon of mountainous areas that involves movement of earth masses from small rockfalls to big rock avalanches and very often produces catastrophic affects. The uncertainty of the frequency and magnitude of the mass movement events has strong impact on human society in terms of life losses and infrastructure damages (Dorren 2003; Holm and Jakob 2009). Unfortunately, the rockfall events are often ignored by the local population due to their relatively low magnitude as compared to the other mass movement process (Holm and Jakob 2009). However, they still pose significant hazard to lives and blockage of the roads. The reason for this impact is primarily human related that includes settlement of human population in mountainous areas at very steep slopes. On the other hand, the major damages occur due to the mass movement volume and long distance travelled from the source point (Corominas 1996). A common problem is to assess the factors and impact of mass movement volume on travel distance.

Previous investigations have analyzed mass movement events and travel distance, using two empirical models: the “Fahrböschung angle” (Heim 1932; Shreve 1968; Scheidegger 1973; Hsü 1975; Corominas 1996; Erismann and Abele 2001) and the “shadow angle” (Lied 1977; Hungr and Evans 1988; Evans and Hungr 1993). Different theories have been proposed to explain the phenomena of long travel distance for the large mass movements (Van Gassen and Cruden 1989; Melosh 1986; Nicoletti and Sorriso-Valvo 1991; Davies et al. 1999). The volume dependence of the Fahrböschung angle has been questioned by many authors for large- (Hsü 1975; Hungr 1990) and small-scale mass movements (Hunter and Fell 2003). There is a lack of agreement between researchers about findings of volume and travel distance relationships. Consequently, different conclusions have been derived from these simple relations.

In Pakistan, like other developing countries, the risk posed by the mass movement before the earthquake of October 8, 2005, was underestimated, and no scientific investigation was carried out. As a result, the people and government had to pay high price in term of human life, property, relocation and reconstruction of settlements. For instance, the Muzaffarabad (the capital of Pakistan-administered Kashmir) and many other important towns and valleys (Jhelum and Neelum valleys) were left isolated due to the disruption of the communication links. Thousands of mass movements were triggered during this earthquake in Muzaffarabad and surrounding areas (Basharat et al. 2014). These were mainly rockfalls, debris falls, rock slides and rock avalanches, ranging in volumes from few hundred cubic meters to hundreds of million cubic meters. The number of fatalities associated directly and indirectly with these mass movements was about 26,500 people (Petley et al. 2006).

Large-volume events with long travel distances occurring during the earthquake were rare but potentially highly destructive. For example, the Hattian Bala rock avalanche having volume more than hundreds of million cubic meters destroyed everything in its travel path through burial and resulted in 595 casualties (Basharat et al. 2012). In addition, this catastrophic event blocked the way of Karli and Tung streams, creating two landslide dams. In contrast, small-volume rockfall events were the most common phenomena during this earthquake (Owen et al. 2008). However, the rockfall events have caused less fatality as compared to large-volume events.

After the devastating effect produced by the mass movements during the earthquake, the efforts are being made to identify and characterize the mass movement event to improve the knowledge about the mass movements through a systematic collection of field data. The information gathered from field data was used to describe the characteristics and

behavior of mass movements such as volume, Fahrböschung angle, fall height, travel path and surface area.

The present study describes the empirical analysis for statistically significant set of data derived from geometric parameters, in Muzaffarabad, Jhelum and Neelum valleys (Fig. 1). The data were analyzed and presented in the form of empirical relationship among the volume, Fahrböschung angle, fall height, travel path and surface area. The consistency of our data was tested by comparing it with data from different parts of the world, published in earlier studies. The analysis indicates the differences in the observed run-out distance and mobility among different types of mass movements. The results may be used to assess and mitigate the risk posed by the mass movements in different part of the world with similar conditions.

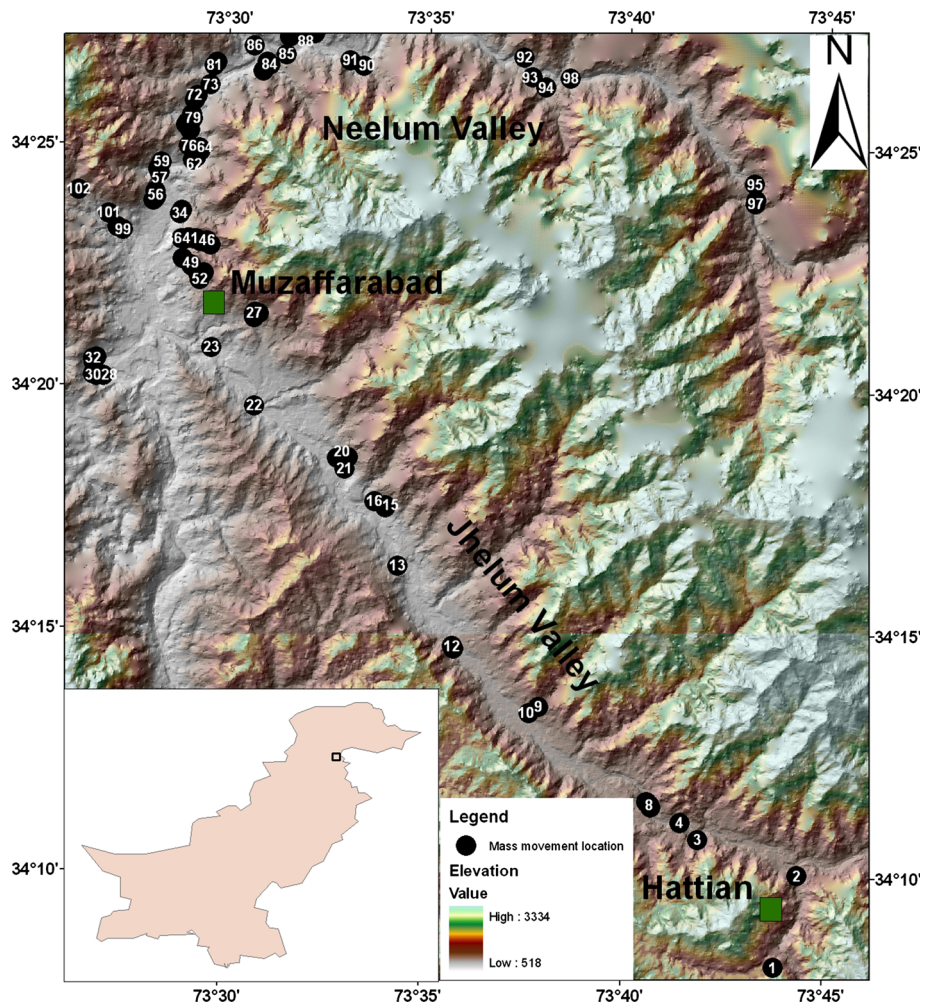


**Fig. 1** Location of the mass movement events, identified for empirical analysis of geometrical parameters of mass movements, triggered by the 2005 Kashmir earthquake in the vicinity of Jhelum Valley, Neelum Valley and Muzaffarabad, in the Northeast Himalayas of Pakistan

1.1 Geographical and geological setting

The 2005 Kashmir earthquake affected area is characterized by young mountains, active tectonics, fragile lithology and steep topography. The area is rugged terrain and mountainous with many old mass movements. The ridges and valleys generally trend southeast–northwest parallel to the regional geological structures of the area. Generally, the relief of

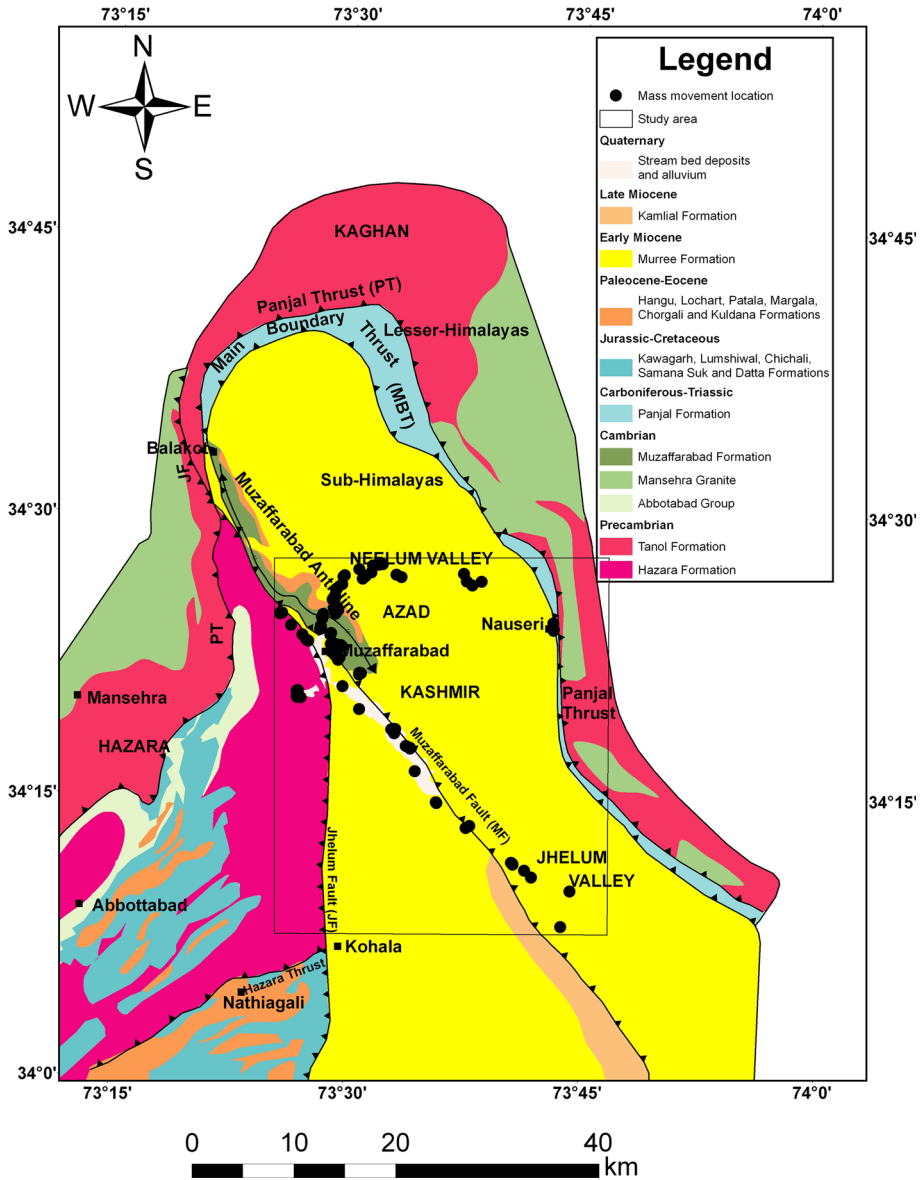


Fig. 2 Geological map of Hazara-Kashmir syntaxis (compiled and modified after Wadia 1931; Calkins et al. 1975; Greco 1989; Baig and Lawrence 1987; Hussain et al. 2004)

the area is high in the northeastern part as compared to southern part (Fig. 1). The weathering of rock depends upon the topography, climatic conditions, geology, structure, vegetation and slopes of the area. Heavy rainfall, high relief, steep slopes and highly sheared and fractured rock units made mass wasting an important degradation process. The degraded talus accumulated on the low foot hills.

Structurally, the region encloses the Hazara-Kashmir syntaxis (HKS). The HKS is a NNW trending regional scale antiform structure that folds the lesser- and sub-Himalayas (Fig. 2). Except for the Himalayan Frontal Thrust, all the major thrusts including Main Boundary Thrust (MBT) and Panjal Thrust (PT) are refolded by this structure. Unlike the usual anticlines, where the younger rocks lie in the limb and older rocks comprises successively in the core, the HKS exposes the youngest rocks in the core and successively older rocks in the limbs (Fig. 2). This explains crustal stacking due to thrusting prior to the formation of the Hazara-Kashmir syntaxial structure (Calkins et al. 1975). Thus, the limbs of the HKS comprise folded PT and MBT. In the HKS, the MBT, PT, Jhelum Fault and Muzaffarabad Fault are the important active tectonic features (Fig. 2; Wadia 1931; Armbruster et al. 1978; Baig and Lawrence 1987; Baig 2006).

The regional geology of the earthquake affected area shows sedimentary, metasedimentary, metavolcanics and metaigneous rock units. These lithostratigraphic units have different geological control on the mass movements of the area. The Precambrian to Tertiary rocks are exposed in the HKS around Muzaffarabad, Jhelum and Neelum valleys areas. The rock sequence includes the Precambrian Hazara and Tanol Formations, the Cambrian Muzaffarabad Formation and Mansehra Granite, the Carboniferous-Triassic Panjal Formation, the Paleocene–Eocene sequence, the Early Miocene Murree Formation, the Late Miocene Kamlial Formation and Quaternary sediments (Fig. 2; Calkins et al. 1975; Greco 1989; Hussain et al. 2004).

The geological units of tertiary sediments comprise of a wide variety of rocks, including alternating nodular limestone, calcareous and carbonaceous shale, sandstone, siltstone, marl, claystone and local conglomerates. The Precambrian Tanol Formation consists of chlorite quartz mica schist, chlorite, biotite quartzofeldspathic schist, metaquartzite, garnet mica schist, graphitic schist and local marble (Shah 1977). The sequence is intruded by early Paleozoic granite gneisses. The rock sequence is multiply deformed and metamorphosed (Greco 1989; Khan 1994). These rocks are jointed and fractured. The Precambrian rocks of Hazara Formation comprise of fractured and cleaved slate, phyllite and shale with minor limestone.

The Carboniferous-Triassic Panjal Formation includes basic metavolcanics, quartzofeldspathic schist and graphitic schist (Khan 1994). The sequence along MBT is highly fractured, jointed and sheared. These lithologies, brittle structures and steep slopes controlled the mass movements locally along MBT during earthquake ground shaking. Most of the mass movements occurred in interbedded sandstone, siltstone, shale and claystone of Murree Formation and highly fractured carbonate rocks of Cambrian Muzaffarabad Formation, which are well known for their susceptibility to mass movement occurrences in many part of the world (;Khazai and Sitar 2003; Chigira et al. 2010). The dolomites of Muzaffarabad Formation along fault are deformed into joints, fractures, breccia and gouge. The sedimentary rocks of sandstone, mudstone, siltstone, shale and claystone are most susceptible to produce shallow mass movements. These are weakly cemented and consequently broken by fractures and joints.

**Table 1** Geometrical data of 103 mass movement events triggered by the 2005 Kashmir earthquake in the vicinity of Jhelum Valley, Neelum Valley and Muzaffarabad in the Northeast Himalayas of Pakistan

S. No	Locations	Type	<i>L</i> (m)	<i>H</i> (m)	<i>D</i> (m)	<i>V</i> (10 <sup>6</sup> m <sup>3</sup> )	Tanz
1	JV1	LRA	2,350	700	60	98.4	0.3
2	Mzd1	LRA	486	355	15	3.105	0.72
3	JV2	LRA	805	460	12	5.76	0.57
4	NV1	LRA	950	600	20	6.75	0.7
5	Mzd2	MRF	650	410	5	0.25	0.62
6	JV3	MRF	800	480	3	0.189	0.6
7	Mzd3	MRF	392	292	6	0.156	0.75
8	Mzd4	MRF	258	150	6	0.138	0.57
9	JV4	MRF	248	187	4	0.128	0.75
10	Mzd5	MRF	625	450	5	0.125	0.72
11	Mzd6	MRF	436	346	4	0.12	0.78
12	Mzd7	MRF	446	290	5	0.12	0.65
13	Mzd8	MRF	206	192	4	0.112	0.93
14	NV2	MRF	266	260	6	0.108	0.96
15	Mzd9	MRF	416	310	4	0.108	0.73
16	Mzd10	MRF	350	282	3	0.105	0.81
17	NV3	MRF	288	248	6	0.102	0.86
18	JV5	MRF	298	238	6	0.102	0.8
19	NV4	MRF	406	306	4	0.100	0.75
20	NV5	MRF	250	228	10	0.100	0.9
21	Mzd11	SRF	230	166	2	0.088	0.72
22	NV6	SRF	570	525	2	0.080	0.93
23	Mzd12	SRF	360	244	5	0.075	0.67
24	Mzd13	SRF	330	274	4	0.072	0.83
25	Mzd14	SRF	364	232	3	0.069	0.64
26	Mzd15	SRF	300	240	1	0.066	0.8
27	Mzd16	SRF	520	332	4	0.06	0.64
28	Mzd17	SRF	248	202	3	0.060	0.81
29	NV7	SRF	230	186	6	0.060	0.8
30	NV8	SRF	252	150	4	0.060	0.6
31	Mzd18	SRF	254	170	2	0.060	0.67
32	JV6	SRF	162	104	5	0.050	0.64
33	JV7	SRF	175	130	5	0.050	0.75
34	Mzd19	SRF	366	290	4	0.044	0.78
35	Mzd20	SRF	306	296	3	0.042	0.96
36	Mzd21	SRF	258	180	4	0.040	0.7
37	NV9	SRF	320	242	3	0.039	0.75
38	Mzd22	SRF	270	156	3	0.036	0.57
39	Mzd23	SRF	256	166	2	0.036	0.64
40	Mzd24	SRF	190	110	3	0.036	0.57
41	NV10	SRF	420	350	5	0.035	0.83
42	Mzd25	SRF	415	315	5	0.035	0.75
43	JV8	SRF	400	300	2	0.032	0.75

**Table 1** continued

S. No	Locations	Type	<i>L</i> (m)	<i>H</i> (m)	<i>D</i> (m)	<i>V</i> (10 <sup>6</sup> m <sup>3</sup> )	Tanz
44	Mzd26	SRF	282	230	3	0.030	0.81
45	NV11	SRF	325	293	5	0.030	0.9
46	NV12	SRF	210	190	3	0.030	0.9
47	NV13	SRF	162	146	4	0.028	0.9
48	NV14	SRF	298	222	2	0.026	0.74
49	Mzd27	SRF	174	122	2	0.022	0.7
50	JV9	SRF	398	300	2	0.022	0.75
51	Mzd28	SRF	270	232	2	0.018	0.86
52	Mzd29	SRF	405	292	2	0.018	0.72
53	Mzd30	SRF	332	206	3	0.018	0.62
54	NV15	SRF	382	326	1	0.018	0.86
55	JV10	SRF	210	126	3	0.018	0.6
56	NV16	SRF	230	240	1	0.017	1.03
57	JV11	SRF	195	116	3	0.016	0.6
58	Mzd31	SRF	144	134	3	0.015	0.93
59	Mzd32	SRF	294	206	3	0.014	0.7
60	NV17	SRF	136	126	2	0.014	0.93
61	NV18	SRF	136	85	2	0.014	0.62
62	Mzd33	SRF	386	282	3	0.012	0.72
63	Mzd34	SRF	160	144	3	0.012	0.9
64	NV19	SRF	202	182	3	0.012	0.9
65	NV20	SRF	180	162	2	0.012	0.9
66	JV12	SRF	140	109	4	0.012	0.78
67	NV21	SRF	446	332	2	0.012	0.75
68	NV22	SRF	196	164	1	0.011	0.83
69	NV23	SRF	150	118	2	0.010	0.78
70	NV24	SRF	132	90	5	0.010	0.67
71	JV13	SRF	110	86	2	0.010	0.78
72	JV14	SRF	208	194	1	0.010	0.93
73	Mzd35	SRF	218	240	3	0.009	1.11
74	NV25	SRF	218	250	2	0.009	1.15
75	NV26	SRF	198	143	3	0.009	0.72
76	Mzd36	SRF	200	166	2	0.009	0.83
77	Mzd37	SRF	350	222	2	0.008	0.62
78	JV15	SRF	86	80	3	0.008	0.93
79	Mzd38	SRF	218	270	3	0.008	1.23
80	NV27	SRF	137	100	2	0.007	0.72
81	NV28	SRF	175	127	2	0.007	0.72
82	JV16	SRF	76	70	5	0.007	0.92
83	Mzd39	SRF	168	151	2	0.007	0.9
84	JV17	SRF	75	70	4	0.007	0.93
85	NV29	SRF	128	106	2	0.006	0.83
86	JV18	SRF	126	109	4	0.006	0.86

**Table 1** continued

S. No	Locations	Type	<i>L</i> (m)	<i>H</i> (m)	<i>D</i> (m)	<i>V</i> (10 <sup>6</sup> m <sup>3</sup> )	Tanz
87	NV30	SRF	354	230	1	0.005	0.64
88	Mzd40	SRF	185	172	2	0.005	0.93
89	JV19	SRF	130	125	3	0.005	0.96
90	JV20	SRF	166	155	2	0.005	0.93
91	JV21	SRF	88	71	2	0.005	0.81
92	JV22	SRF	94	90	4	0.005	0.96
93	JV23	SRF	100	86	1	0.004	0.86
94	JV24	SRF	112	121	1	0.004	1.08
95	Mzd41	SRF	98	86	2	0.004	0.83
96	NV31	SRF	126	86	3	0.003	0.68
97	NV32	SRF	124	104	2	0.003	0.86
98	NV33	SRF	330	250	1	0.003	0.75
99	NV34	SRF	254	350	1	0.003	1.37
100	JV25	SRF	232	200	3	0.002	0.86
101	Mzd42	SRF	110	163	3	0.002	1.48
102	NV35	SRF	120	160	2	0.002	1.33
103	Mzd43	SRF	178	110	2	0.002	0.62

LRA, large rockfall; MRF, medium rockfall; SRF, small rockfall; *L*, travel distance; *H*, height of fall; *D*, estimated depth; Tanz, tangent of Fahrböschung angle; *V*, volume; JV, Jhelum Valley; NV, Neelum Valley; Mzd, Muzaffarabad

## 2 Data source and methodology

Systematic field investigations were carried out to identify mass movement events. A total of 103 mass movement events were identified, and detailed surveys were carried out to gather field data for analysis (Fig. 1). These mass movements were mapped during field investigations in November 2010–2011. A mass movement inventory, containing the geometric parameters including volume, length, height, surface area, deposit area and Fahrböschung angle, was prepared for statistical analysis (Table 1). This inventory also indicates the locations and types of 103 mass movement events (Fig. 3).

The longitudinal profiles that describe the geometrical parameters of each mass movement event were prepared. Length (travel distance) and height (fall height) were measured from the longitudinal profiles. In addition, Fahrböschung angle was measured directly in the field and later on verified from the longitudinal profiles. ArcGIS 9.3 software was used to measure the surface area of polygons that represent the mass movement and include source, path and deposit. In order to calculate the volume of mass movements, the average thickness was estimated for the deposit volume. The best way to estimate mass movement volume is analysis of change in elevation using pre- and post-earthquake digital elevation models (DEMs; Kerle 2002; Martha et al. 2010). However, due to the scarcity of pre- and post-earthquake DEMs, our measurement of volume is mainly based on the field assessment (e.g., Legros 2002; Devoli et al. 2009). For this study, the volumes of the mass movements were estimated by multiplying the deposit area with an estimated average thickness (estimated on the basis of field observation). In some cases, the volumes of the mass movement events that occurred along the Jhelum River and the Neelum River were smaller than the actual rock mass displaced from the scarp. This difference in volume is



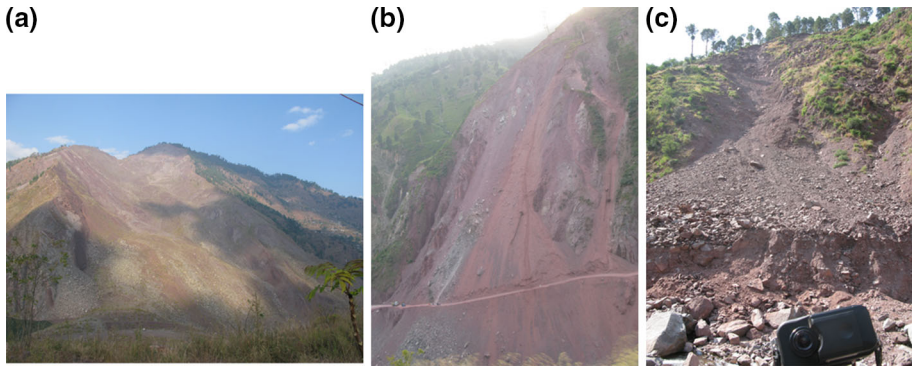


**Fig. 3** Photographs show the types, locations and parameters of mass movement (a) deep-seated large rockfall (Hattian Bala), (b) Dunga Kuss rockfall (road in Neelum Valley), (c) small rockfall (Panjgran, Neelum Valley)

attributed to erosion of the deposited material by the river, especially during flooding. However, these differences are more likely to have minor effect on the validity and reliability of the data. For mass movements with small volumes, it is sometimes difficult to estimate the accurate volume due to hindrances like dense vegetation and subsequent transportation of the material. In these cases, the minimum estimate for the volume was taken into account (e.g., Legros 2002).

### 3 Types of investigated mass movements

A classification based on a volumetric nomenclature (Varnes 1978; Fell 1994) for rockfall was followed to describe all types of mass movement data, collected during field surveys, because our primary concern of rockfall classification involves travel distance and Fahr-böschung angle to explain the manner of progression of movement. The present rockfall size classification based on a volumetric nomenclature was used for the empirical analysis (Table 2).

The term rockfall is characterized by the failure of relatively steep rock slopes or cliffs along a surface where little or no shear displacement takes place (Varnes 1978). In general, rockfalls involve a direct downward movement and large to small detachments ( $10^2$ –

**Table 2** Mass movement classification based on a volumetric nomenclature (modified after Varnes 1978; Fell 1994)

Types of falls	Volume (m <sup>3</sup> )	Description
Small rockfall	<10 <sup>4</sup>	A large block or more than one block which may fragment during travel
Medium rockfall	10 <sup>4</sup> –10 <sup>6</sup>	Free falling of rock blocks of different size or detached from the rock slope
Large rockfall	>10 <sup>6</sup>	Falls of large volume to facilitate the very rapid flow of rock or debris, which may travel a considerable distance

$10^8 \text{ m}^3$ ), although there is no well-defined volume limit (Evans and Hungr 1993). The low-magnitude rockfall ( $<10^4 \text{ m}^3$ ) termed as small rockfall or debris fall (Varnes 1978) is distinguished from a medium rockfall ( $10^4\text{--}10^6 \text{ m}^3$ ). Subsequently, medium rockfall is distinguished from large rockfall ( $>10^6 \text{ m}^3$ ). Large rockfalls ( $>10^6 \text{ m}^3$ ) are termed as mountain fall or sturzstrom (Heim 1932) or rock avalanche (Varnes 1978).

#### 4 Geometrical parameters considered for empirical analysis

In this study, the geometrical parameters considered for the empirical analysis are related to the mass movement failure as shown in Fig. 4. One empirical parameter is the Fahrböschung angle (Heim 1932) or travel angle. The Fahrböschung is the angle between the horizontal and line connecting from the highest point of the mass movement scarp to the distal margin of the displaced mass. Various scientists have referred to this line by other names such as: angle of the equivalent coefficient of friction (Shreve 1968), travel angle (Hungr 1990; Cruden and Varnes 1996), reach angle (Corominas 1996) and travel distance angle (Hunter and Fell 2003).

The term  $L$  refers to the travel distance or corresponding horizontal distance which is the horizontal projection of the line connected from the source point of the mass movement and the farthest block. The term  $H$  is the fall height or elevation difference between the highest point and the lowest point of the mass movement.

#### 5 Data analysis

##### 5.1 Relationship between volume and Fahrböschung angle for mass movements

The plot of the Fahrböschung angle versus mass movement volume in Fig. 5 shows inverse correlation between the tangent of the Fahrböschung values and mass movement volumes.

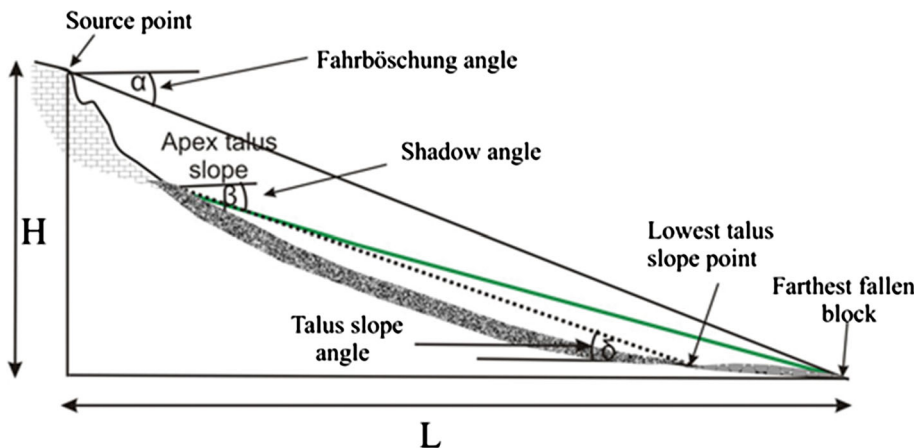


**Fig. 4** Sketch of mass movement source point, falling mass and deposit. Definitions of parameters used in the present analysis are explained in text. Sketch is modified from Evans and Hungr (1993) and Copons et al. (2009)

A regression equation has been obtained,  $\text{Log tan}\alpha = -0.066 \log V - 0.210$ , with a squared correlation ( $R^2 = 0.29$ ), which estimates the maximum travel distance of mass movement events from their volume. The relationship between mass movement volume and Fahrböschung angle suggests that the values of the Fahrböschung angle decrease with the increase in volume of the mass movement events. However, in some cases, small-volume mass movements have Fahrböschung angles as low as the large-volume mass movements (Table 1; Fig. 5). The non-uniformity of mass movements is apparent in scattered diagram where data points corresponding to landslide volume and travelled distance are widely dispersed along regression line (Fig. 5).

5.2 Relationship between the volume and Fahrböschung angle for individual groups of mass movements

To understand the effect of volume on Fahrböschung angle for each individual group of rockfalls, the data set of 103 mass movement events was split into large, medium and small rockfalls based on the volume of the mass movements (Varnes 1978; Fell 1994; Table 2).

The tangent of the Fahrböschung values was plotted against the volumes of each individual group of large, medium and small rockfalls in a log–log plot (Fig. 6). The coefficient of regression analysis for each individual group (large, medium and small) and their statistical information are presented in Table 3. The analysis shows the linear trend and an existing minor correlation between the tangent of the Fahrböschung values and the volume of the group of all mass movements (Fig. 6; Table 3). For the analysis of the large rockfall group, unfortunately, only four large rockfalls were available which posed limitation in statistical analysis of the group of rockfalls. To analyze the medium rockfall

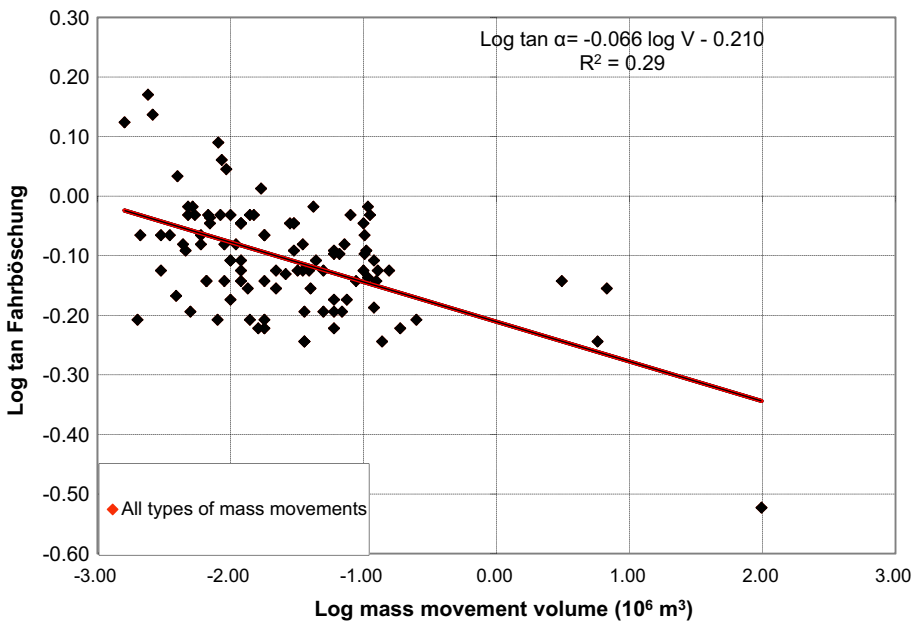
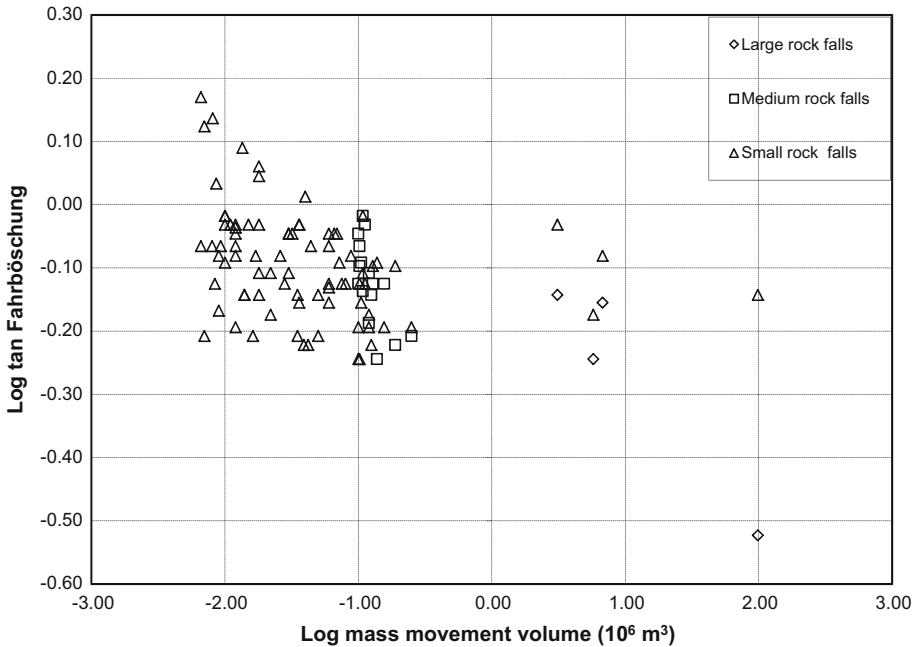


Fig. 5 Relationship between log tangent of the Fahrböschung and log mass movement volume for all investigated mass movements triggered by the 2005 Kashmir earthquake



**Fig. 6** Relationship between tangent of the Fahrböschung and volume for large, medium and small rockfalls

group, 16 rockfalls having volume  $10^4$ – $10^6$  m<sup>3</sup> were taken into account for analysis. The analysis shows that there is a significant and a good correlation between the volume and Fahrböschung angle values (Table 3). On the other hand, 83 small rockfalls with smallest volumes ( $<1 \times 10^4$ ) were considered for the analysis of the small rockfall group. The result indicates that there is a statistically significant but minor correlation between the tangent of the Fahrböschung angle and the small rockfalls (Table 3). The analyses show that mobility increases with increasing volume of mass movement.

5.3 Relationship between the height of fall (*H*) and the travel distance (*L*)

The analysis of 16 medium rockfalls and 83 small rockfalls was performed to determine the relationship between height of fall and travel distance (Tables 1 and 2). The values of

**Table 3** Results of the linear regression analysis of tan $\alpha$  versus the mass movement volume of each individual group

Mass movement types	<i>N</i>	<i>V</i>	<i>r</i>	<i>r</i> <sup>2</sup>	SE	Sig.	Comments
All mass movements	103	0.002–0.98	0.54	0.29	0.07	0.000	Minor correlation
Large rockfalls	4	1.3–98.0	0.96	0.93	0.05	0.03	Strong correlation
Medium rockfalls	16	0.1–0.25	0.67	0.45	0.05	0.004	Good correlation
Small rockfalls	83	0.002–0.01	0.42	0.17	0.07	0.000	Minor correlation

*N*, number of mass movements; *V*, volume in million m<sup>3</sup>; *r*, correlation; *r*<sup>2</sup>, coefficient of determination; SE, standard error; Sig., significant

height of fall ( $H$ ) versus travel distance ( $L$ ) were plotted on a log–log plot (Figs. 7, 8). For the data set of 16 medium rockfall events (Fig. 7), the standard least square regression analysis gives the empirical relationship:  $\text{Log } L = 1.138 \text{ log } H - 0.219$ , with squared correlation  $R^2 = 0.86$ . For the data set of 83 small rockfall events (Fig. 8), a best fit regression equation is obtained:  $\text{Log } L = 0.953 \text{ log } H + 0.195$ , with squared correlation  $R^2 = 0.83$ .

An analysis of the data shows that the travel distance is proportional to the height of fall for both types (medium rockfalls and small rockfalls) of mass movements (Figs. 7, 8). This indicates that there is a significant positive relationship and linear trend between the height of the fall and travel distance for medium rockfalls ( $R^2 = 0.86$ ) and small rockfalls ( $R^2 = 0.83$ ). In addition, the fall height does not affect the Fahrböschung angle values in this analysis because different values of the tangent of the Fahrböschung were found for similar fall height (Table 4).

#### 5.4 Relationship between surface area and volume of mass movements

In general, the larger surface area of a mass movement is likely to have larger volume. An analysis of 103 mass movement events was performed to determine the relationship between the volume and surface area. Figure 9 shows the values of the different surface areas and their respective volumes plotted on a log–log graph. The best fit equation obtained from the least square regression analysis is:  $\text{Log } A = 0.584 \text{ log } V + 1.0537$ , with squared correlation  $R^2 = 0.79$ .

An analysis of the data reveals that there is statistically significant positive correlation ( $R^2 = 0.79$ ) between the surface area and the volume of the mass movements. This

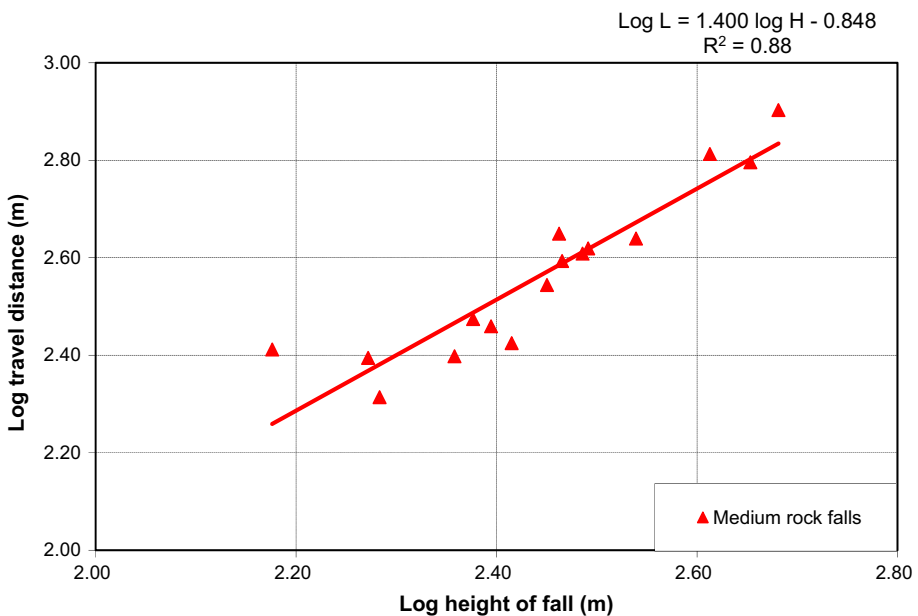


**Fig. 7** Relationship between the log height of the fall ( $H$ ) and the log travel distance ( $L$ ) for all 16 types of medium rockfalls triggered by the 2005 Kashmir earthquake

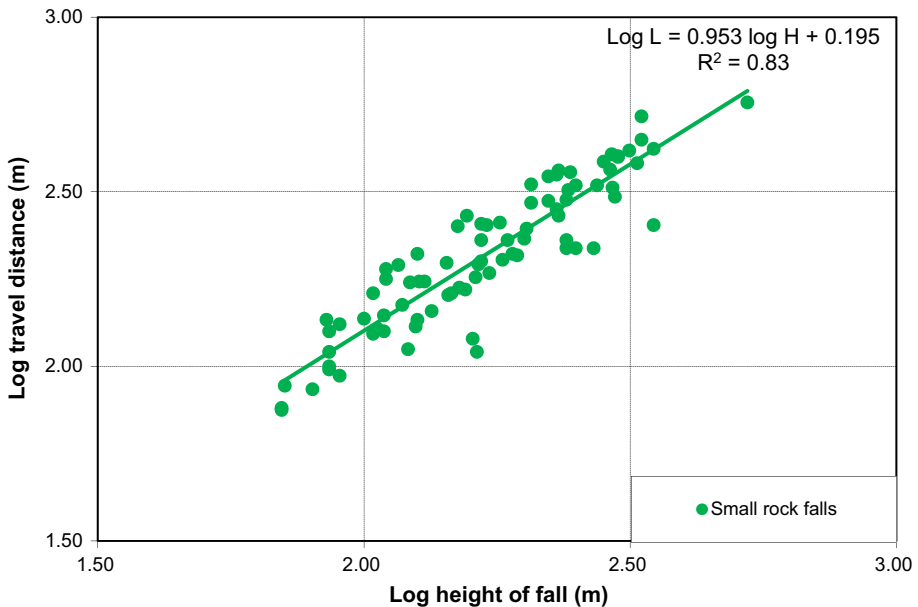


**Fig. 8** Relationship between the log height of fall ( $H$ ) and the log travel distance ( $L$ ) for all 83 types of small rockfalls triggered by the 2005 Kashmir earthquake

indicates that the volume of the mass movements is directly proportional to the surface area.

### 5.5 Relationship between volume and Fahrböschung angle for degree of confinement

The term confined was used for those failure surfaces that travel deep under the original ground and deposited the material at foot in the form of bulging. Conversely, the term unconfined was used when the material deposited below the valley bottom without apparent foot bulging. In order to determine the effect of the degree of confinement on mass movement travel distance, travel path was divided into unconfined, partly confined and confined travel paths. The Fahrböschung angle values versus volume of unconfined, partly confined and confined mass movements were plotted on log–log plot (Fig. 10). The analysis for each degree of confinement (unconfined, partly confined and confined) and their statistical information are presented in Table 5. The results indicate that no correlation was found for confined travel path and minor correlation was found for the unconfined and partly confined travel paths.

## 6 Comparison between present and published data

In order to understand the consistency of the 2005 Kashmir earthquake data set with those published in earlier studies in the different parts of the world. The data published in several references were collected and plotted on a log–log graph (Fig. 11). The analysis shows the relationship between the Fahrböschung angle and volume of the mass movements for rock

**Table 4** Geometrical data of similar height of fall with different Fahrböschung angle

S. No	Type	<i>L</i> (m)	<i>H</i> (m)	Tanz
1	MRF	392	292	0.75
2	MRF	258	150	0.57
3	MRF	446	290	0.65
4	MRF	350	282	0.81
5	SRF	230	166	0.72
6	SRF	300	240	0.8
7	SRF	520	332	0.64
8	SRF	252	150	0.6
9	SRF	162	104	0.64
10	SRF	366	290	0.78
11	SRF	256	166	0.64
12	SRF	190	110	0.57
13	SRF	420	350	0.83
14	SRF	400	300	0.75
15	SRF	282	230	0.81
16	SRF	298	222	0.74
17	SRF	398	300	0.75
18	SRF	405	292	0.72
19	SRF	332	206	0.62
20	SRF	210	126	0.6
21	SRF	230	240	1.03
22	SRF	294	206	0.7
23	SRF	136	126	0.93
24	SRF	386	282	0.72
25	SRF	446	332	0.75
26	SRF	218	240	1.11
27	SRF	200	166	0.83
28	SRF	350	222	0.62
29	SRF	354	230	0.64
30	SRF	100	86	0.86
31	SRF	98	86	0.83
32	SRF	126	86	0.68
33	SRF	124	104	0.86
34	SRF	254	350	1.37
35	SRF	178	110	0.62

MRF, medium rockfall; SRF, small rockfall; *L*, travel distance; *H*, height of fall; Tanz, tangent of Fahrböschung angle

avalanches and rockfalls from the previously published data (Scheidegger 1973; Erismann and Abele 2001; Copons et al. 2009) and the 2005 Kashmir earthquake data set. Despite the diversity of the data set and the differing mechanisms, the results showed a decreasing tendency of Fahrböschung angle ( $\tan\alpha$ ) with increasing mass movement volume. This indicates that the volume of the mass movement has a strong effect on travel distance (Fig. 11).

As shown in Fig. 11, most of the scattered data near the left top of the plot belong to the small rockfalls of Copons et al. (2009). The representative points for large rock avalanches

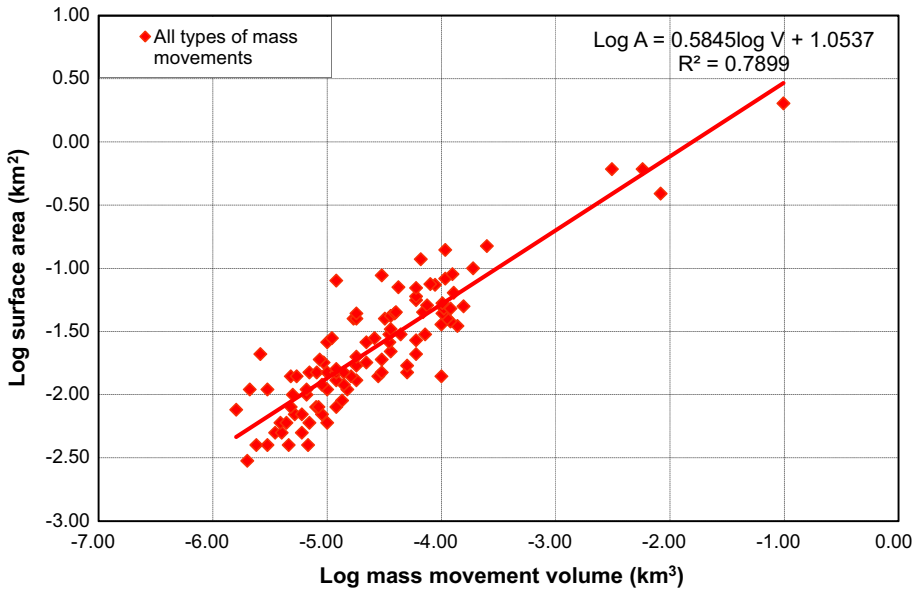


**Fig. 9** Relationship between log surface area and log mass movement volume for all types of mass movements triggered by the 2005 Kashmir earthquake

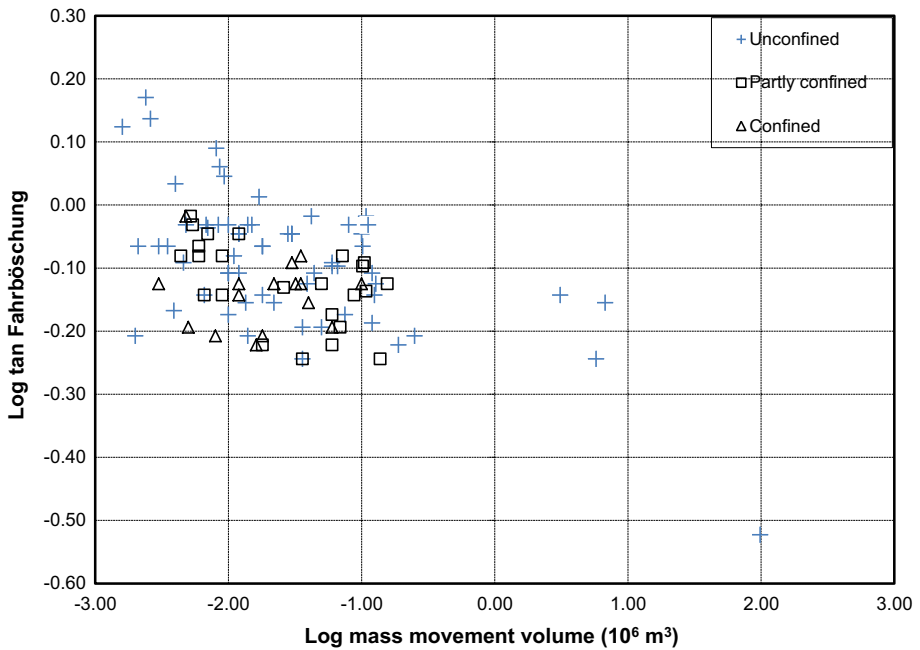


**Fig. 10** Relationship between tangent of the Fahrböschung and volume for degree of confinement



**Table 5** Results of the linear regression analysis of  $\tan\alpha$  versus volume for unconfined, partly confined and confined mass movements

Mass movement types	<i>N</i>	<i>r</i>	<i>r</i> <sup>2</sup>	SE	Sig.	Comments
Unconfined	63	0.61	0.37	0.083	0.000	Minor correlation
Partly confined	24	0.53	0.25	0.056	0.008	Minor correlation
Confined	16	0.02	0.001	0.07	0.94	No correlation

*N*, number of mass movements; *r*, correlation; *r*<sup>2</sup>, coefficient of determination; SE, standard error; Sig., significant

(Scheidegger 1973; Erismann and Abele 2001) are concentrated in the lower right part of the plot. Due to larger volumes, these rock avalanches possess low  $\tan\alpha$  values which significantly reduce scatter in the plot. The 2005 Kashmir earthquake data set involves mass movements with different volumes from small rockfalls to large rockfalls. The points are concentrated in the middle of the plot. This means that mass movements with smaller volumes are on the top left area of the plot and the mass movements with high volumes are in the lower right part of the plot.

The 2005 Kashmir earthquake data set shows the higher values of the Fahrböschung angle similar to Copons et al.’s (2009) data set, while the data set of Scheidegger (1973) and Erismann and Abele (2001) shows the lower values of the Fahrböschung angle. This is due to the smaller volume of the rockfalls of the 2005 Kashmir earthquake data set which

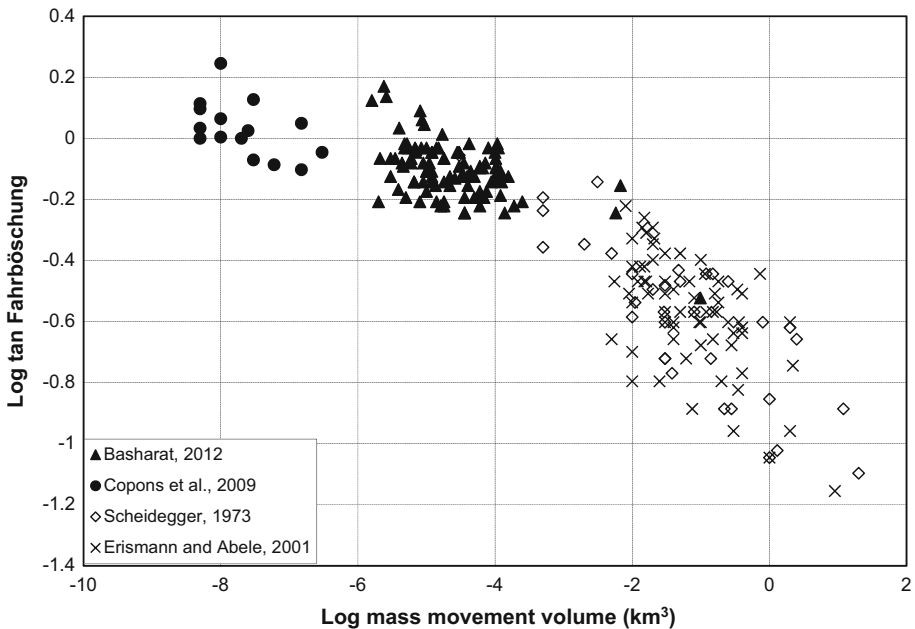


**Fig. 11** Relationship between log tangent of the Fahrböschung and log mass movement volume. Comparison between the data of Scheidegger (1973), Erismann and Abele (2001), Copons et al. (2009) and the 2005 Kashmir earthquake data set

have a different dynamic motion than larger rockfalls ( $>10^6 \text{ m}^3$ ), as already accepted by many researchers (Nicoletti and Sorriso-Valvo 1991; Corominas 1996; Erismann and Abele 2001).

The analysis of the 2005 Kashmir earthquake data set reveals that there is weak or minor correlation ( $R^2 = 29$ ) between volume of mass movement and Fahrböschung angle ( $\tan\alpha$ ), while those plotted by Scheidegger (1973) and Copons et al. (2009) have coefficients of correlation ( $R^2$ ) ranging from 0.73 to 0.49. However, there is not much difference of correlation ( $R^2 = 0.35$ ) for the data set of Erismann and Abele (2001) and for large scale mass movements. Based on the observation of the different data sets, it can be concluded that the empirical relationship suggested in earlier studies is mainly consistent with the data set of the 2005 Kashmir earthquake. However, the 2005 Kashmir earthquake data set displays higher values of Fahrböschung angle as compared to the previous published data except Copons et al. (2009) data set. The higher values of Fahrböschung angle in the data set belong to the smaller volume of the rockfalls. Moreover, these rockfalls occurred mainly nearby rivers, streams, roads and on high-altitude areas.

## 7 Conclusions

This study presents empirical relationships for better understanding of mass movement behavior in the vicinity of the Muzaffarabad and surrounding areas, in the Northeast Himalayas of Pakistan. Based on the field data, different types of mass movements with similar mechanisms of failures were considered for this analysis. The relationship between different parameters including volume, Fahrböschung angle, fall height, surface area, travel path and mass movement travel distance was analyzed. The empirical analysis showed that the Fahrböschung angle depends to some extent on the volume. Furthermore, minor correlation was found between the Fahrböschung angle and volumes of small rockfalls. A linear trend with strong correlation exists between height of fall and travel distance for medium rockfalls ( $R^2 = 0.86$ ) and small rockfalls ( $R^2 = 0.83$ ). For this data set, height of fall does not affect the Fahrböschung angle values, because for similar height of fall, different values of the Fahrböschung angle were found. Moreover, for the analysis of degree of confinement, minor correlation was found for unconfined and partly confined travel paths, and no correlation was found for confined travel path. The empirical results of the 2005 Kashmir earthquake data set are mainly consistent with the previously published data from other parts of the world.

**Acknowledgments** We would like to acknowledge the University of Azad Jammu and Kashmir Muzaffarabad, which has funded the research under Faculty Development Programme. We would also like to acknowledge Director, Institute of Geology, for providing transportation during field work. We offer our special thanks to anonymous reviewers for their helpful comments.

## References

- Armbruster J, Seeber L, Jacob KB (1978) The northwestern termination of the Himalayan mountain front: active tectonics from micro earthquakes. *J Geophys Res* 83:269–282
- Baig MS (2006) Active faulting and earthquake deformation in Hazara-Kashmir Syntaxis, Azad Kashmir, northwest Himalaya, Pakistan. In: Kausar AB, Karim T, Khna T (eds) Extended abstracts, international conference on 8 October 2005 earthquake in Pakistan: its implications and hazard mitigation. Geological Survey of Pakistan, Islamabad pp 27–28

- Baig MS, Lawrence RD (1987) Precambrian to early Paleozoic orogenesis in the Himalaya. *Kashmir J Geol* 5:1–22
- Basharat M, Rohn J, Baig MS, Ehret D (2012) Lithological and structural control of Hattian Bala rock avalanche triggered by the Kashmir earthquake 2005, NW Himalaya, Pakistan. *J Earth Sci* 23(2):213–224
- Basharat M, Rohn J, Baig MS, Khan MR (2014) Spatial distribution analysis of mass movements triggered by the 2005 Kashmir earthquake in the Northeast Himalayas of Pakistan. *J Geomorphol* 206:203–214
- Calkins JA, Offield TW, Abdullah SKM, Ali ST (1975) Geology of the Southern Himalaya in Hazara, Pakistan, and adjacent areas. *US Geol Surv Prof Pap* 716-C:29
- Chigira M, Wu X, Inokuchi T, Wang G (2010) Landslides induced by the 2008 Wenchuan earthquake, Sichuan, China. *Geomorphology* 118:225–238
- Copons R, Vilaplana JM, Linares R (2009) Rock fall travel distance analysis by using empirical models (Sol'a d'Andorra la Vella, Central Pyrenees). *Nat Hazards Earth Syst Sci* 9:2107–2118
- Corominas J (1996) The angle of reach as a mobility index for small and large landslides. *Can Geotech J* 33:260–271
- Cruden DM, Varnes DJ (1996) Landslide types and processes. In: Turner AK, Schuster RL (eds) *Special report in landslides investigation and mitigation*, vol 247. pp 36–75
- Davies TRH, McSaveney MJ, Hodgson KA (1999) A fragmentation spreading model for long runout rock avalanches. *Can Geotech J* 36(6):1096–1110
- Devoli G, Blasio FV, Elverhøi A, Høeg K (2009) Statistical analysis of landslide events in Central America and their run-out distance. *Geotech Geol Eng* 27(1):23–42
- Dorren L (2003) A review of rockfall mechanics and modelling. *Prog Phy Geog* 27(1):69–87
- Erismann T, Abele G (2001) *Dynamics of rockslides and rock falls*. Springer, Berlin, p 316
- Evans SG, Hungr O (1993) The assessment of rock fall hazard at the base of talus slopes. *Can Geotech J* 30:620–636
- Fell R (1994) Landslide risk assessment and acceptable risk. *Can Geotech J* 31(2):261–272
- Greco A (1989) Tectonic and metamorphism of the western Himalayan Syntaxis area (Azad Kashmir NE Pakistan). Dissertation ETH Zurich 8779: 1–113
- Heim A (1932) *Bergsturz und Menschenleben*. Beiblatt zur Viertel-jahresschrift der Naturforschenden Gesellschaft in Zurich 225–230
- Holm K, Jakob M (2009) Long rockfall runout, Pascua Lama, Chile. *Can Geotech J* 46:225–230
- Hsü KJ (1975) Catastrophic debris streams (Sturzstroms) generated by rock falls. *Am Bull* 86:129–140
- Hungr O (1990) Mobility of rock avalanches. Report of the National Institute for Earth Science and Disaster Prevention 46:11–20
- Hungr O, Evans SG (1988) Engineering evaluation of fragmental rock fall hazards. In: *Engineering evaluation of fragmental rock fall hazards, proceedings 5th international symposium on landslides*. Lausanne, pp 685–690
- Hunter G, Fell R (2003) Travel distance angle for “rapid” landslides in constructed and natural soil slopes. *Can Geotech J* 40:1123–1141
- Hussain A, Iqbal S, Nasir S (2004) Geological maps of the Garhi Habibullah and Nauseri area, District Muzaffarabad, AJK: Geol. Surv Pak Prelim Map Ser VI(14), Sheet No. 43 F/7,11, 1:50,000
- Kerle N (2002) Volume estimation of the 1998 flank collapse at Casita volcano, Nicaragua: a comparison of photogrammetric and conventional techniques. *Earth Surf Process Landforms* 27(7):759–772
- Khan MS (1994) Petrology and geochemistry of the Panjal volcanics in the Azad Kashmir and Kaghan areas of the NW Himalaya. PhD thesis, University of Punjab, Pakistan, p 270
- Khazai B, Sitar N (2003) Evaluation of factors controlling earthquake-induced landslides caused by Chi–Chi earthquake and comparison with the Northridge and Loma Prieta events. *Eng Geol* 71:79–95
- Legros F (2002) The mobility of long-runout landslides. *Eng Geol* 63(3):301–331
- Lied K (1977) Rockfall problems in Norway. In: *Rockfall dynamics and protective work effectiveness*, vol 90. Instituto Sperimentale Modelli e Structure (ISMES), Bergamo, Italy, pp 51–53
- Martha TR, Kerle N, Jetten V, van Westen CJ, Kumar KV (2010) Landslide volumetric analysis using Cartosat-1-derived DEMs. *Geosci Remote Sens Lett IEEE* 7(3):582–586
- Melosh HJ (1986) The physics of very large landslides. *Acta Mech* 64:89–99
- Nicoletti PG, Sorriso-Valvo M (1991) Geomorphic controls of the shape and mobility of rock avalanches. *Geol Soc Am Bulletin* 103:1365–1373
- Owen LA, Kamp U, Khattak GA, Harp EL, Keefer DK, Bauer MA (2008) Landslides triggered by the 8 October 2005 Kashmir earthquake. *Geomorphology* 94:1–9
- Petley D, Dunning S, Rosser N, Kausar AB (2006) Incipient Landslides in the Jhelum valley, Pakistan following the 8th October 2005 earthquake. *Disaster Mitigation of Rock Flows, Slope failures and Landslides by Universal Academy Press*: 1–9

- Scheidegger A (1973) On the prediction of the reach and velocity of catastrophic landslides. *Rock Mech* 5:231–236
- Shah SMI (1977) Stratigraphy of Pakistan. *Geol Surv Pak Mem* 12:1–138
- Shreve RL (1968) The black hawk landslide. *Geol Soc Am Spec Pap* 108:47
- Van Gassen W, Cruden D (1989) Momentum transfer and friction in the debris rock avalanches. *Can Geotech J* 26:623–628
- Varnes DJ (1978) Slope movement types and processes. In: Schuster RL, Krizek RJ (eds) Special report 176: landslides: analysis and control. Transportation and Road Research Board National Academy of Science, Washington DC, pp 11–33
- Wadia DN (1931) The syntaxis of the north–west Himalaya-its rocks, tectonics, and orogeny. *Rec Geol Surv India* 65:189–220